

Equations for the soil-water characteristic curve

D.G. FREDLUND AND A. XING

Department of Civil Engineering, University of Saskatchewan, 57 Campus Drive, Saskatoon, SK, Canada S7N 5A9.

Reproduced with permission from, *Canadian Geotechnical Journal*, 31(3): 521-532, 1994.

Received July 27, 1993

Accepted March 7, 1994

The soil-water characteristic curve can be used to estimate various parameters used to describe unsaturated soil behaviour. A general equation for the soil-water characteristic curve is proposed. A nonlinear, least-squares computer program is used to determine the best-fit parameters for experimental data presented in the literature. The equation is based on the assumption that the shape of the soil-water characteristic curve is dependent upon the pore-size distribution of the soil (i.e., the desaturation is a function of the pore-size distribution). The equation has the form of an integrated frequency distribution curve. The equation provides a good fit for sand, silt, and clay soils over the entire suction range from 0 to 10^6 kPa.

Key Words: soil-water characteristic curve, pore-size distribution, nonlinear curve fitting, soil suction, water content.

La courbe caractéristique sol-eau peut être utilisée pour estimer divers paramètres décrivant le comportement d'un sol non saturé. On propose ici une équation pour cette courbe caractéristique sol-eau. Un programme non linéaire, par moindres carrés, est utilisé pour déterminer les paramètres qui permettent d'approcher au mieux les données expérimentales recueillies dans la littérature. L'équation est basée sur l'hypothèse que la forme de la courbe caractéristique sol-eau dépend de la répartition de la taille des pores du sol (à savoir que la perte de saturation est une fonction de cette répartition). L'équation a la forme d'une intégrale de courbe de répartition de fréquences. Cette équation permet un bon ajustement pour les sols sableux, silteux et argileux sur toute la gamme des valeurs de succion, de 0 à 10^6 kPa.

Mots clés : courbe caractéristique sol-eau, répartition de la taille des pores, ajustement non linéaire, succion dans le sol, teneur en eau.

[Traduit par la rédaction]

Can. Geotech. J. 31, 521-532 (1994)

Introduction

A theoretical framework for unsaturated soil mechanics has been established over the past two decades. The constitutive equations for volume change, shear strength, and flow through unsaturated soil have become generally accepted in geotechnical engineering (Fredlund and Rahardjo 1993a). The measurement of soil parameters for the unsaturated soil constitutive models, however, remains a demanding laboratory process. For most practical problems, it has been found that approximate soil properties are adequate for analysis (Papagiannakis and Fredlund 1984). Hence, empirical procedures to estimate unsaturated soil-parameters would be valuable.

Laboratory studies have shown that there is a relationship between the soil-water characteristic curve for a particular soil and the properties of the unsaturated soil (Fredlund and Rahardjo 1993b). For example, it has become an acceptable procedure to predict empirically the permeability function for an unsaturated soil by using the saturated coefficient of permeability and the soil-water characteristic curve (Marshall 1958; Mualem 1986; University of Saskatchewan 1984). Similar procedures have been suggested for the shear strength properties of an unsaturated soil (Fredlund and Rahardjo 1993b). Since the soil-water characteristic curve is used as the basis for the prediction of other unsaturated soil parameters, such as the permeability and shear-strength functions, it is important to have a reasonably accurate characterization of the soil-water characteristic curve.

This paper reviews the forms of mathematical equations that have been suggested to characterize the soil-water characteristic curve. It appears that none of the suggested equations accurately fit laboratory data over the entire suction

range. This paper proposes a new equation that can be used to fit laboratory data over the entire soil suction range. A mathematical basis for the equation is described and a best-fit procedure is outlined to obtain the parameters for the equation.

Definitions¹

The soil-water characteristic curve for a soil is defined as the relationship between water content and suction for the soil (Williams 1982). The water content defines the amount of water contained within the pores of the soil. In soil science, volumetric water content, θ , is most commonly used. In geotechnical engineering practice, gravimetric water content, w , which is the ratio of the mass of water to the mass of solids, is most commonly used. The degree of saturation, S , is another term commonly used to indicate the percentage of the voids that are filled with water. The above variables have also been used in a normalized form where the water contents are referenced to a residual water content (or to zero water content).

The suction may be either the matric suction (also known as capillary pressure) of the soil (i.e., $u_a - u_w$, where u_a is the pore-air pressure and u_w is the pore-water pressure) or total suction (i.e., matric plus osmotic suction). At high suc-

¹There are several soil terms that are used interchangeably in the literature. The terminology used in the paper is most consistent with that found in the geotechnical literature. Other terms are used in the geo-environmental, petroleum, and some of the soil science disciplines. Some of these equivalences are as follows: matric suction \equiv capillary pressure, air-entry value \equiv displacement pressure, and soil-water characteristic curve \equiv suction -- volumetric water content curve.

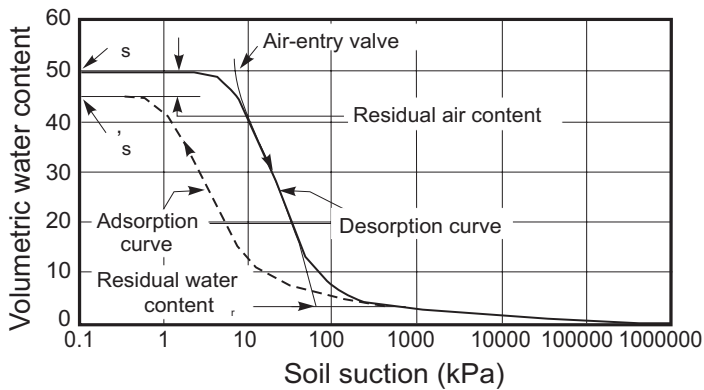


FIG. 1. Typical soil-water characteristic for a silty soil

tions (i.e., greater than about 1500 kPa), matric suction and total suction can generally be assumed to be equivalent.

As a result of the different terminologies used, the soil-water characteristic curves have taken on numerous forms. It is suggested that the term soil-water characteristic curve be used to represent the relationship between volumetric water content, θ , and matric suction. Volumetric water content test results in the low suction range are often presented using an arithmetic scale. Soil-water characteristic curves over the entire suction range are often plotted using a logarithmic scale.

Figure 1 shows a typical plot of a soil-water characteristic curve for a silty soil, along with some of its key characteristics. The air-entry value of the soil (i.e., bubbling pressure) is the matric suction where air starts to enter the largest pores in the soil. The residual water content is the water content where a large suction change is required to remove additional water from the soil. This definition is vague and an empirical procedure for its quantification would be useful. A consistent way to define the residual water content is shown in Fig. 1. A tangent line is drawn from the inflection point. The curve in the high-suction range can be approximated by another line. The residual water content θ_r can be approximated as the ordinate of the point at which the two lines intersect (Fig. 1). The total suction corresponding to zero water content appears to be essentially the same for all types of soils. A value slightly below 10^6 kPa has been experimentally supported for a variety of soils (Croney and Coleman 1961). This value is also supported by thermodynamic considerations (Richards 1965). In other words, there is a maximum total suction value corresponding to a zero relative humidity in any porous medium.

The main curve shown in Fig. 1 is a desorption curve. The adsorption curve differs from the desorption curve as a result of hysteresis. The end point of the adsorption curve may differ from the starting point of the desorption curve because of air entrapment in the soil. Both curves have a similar form; however, this paper primarily considers the desorption curve.

Typical soil-water characteristic curves (i.e., desorption curves) for different soils are shown in Fig. 2. The saturated water content, θ_s , and the air-entry value or bubbling pressure, $(u_a - u_w)_b$, generally increase with the plasticity of the soil. Other factors such as stress history also affect the shape of the soil-water characteristic curves.

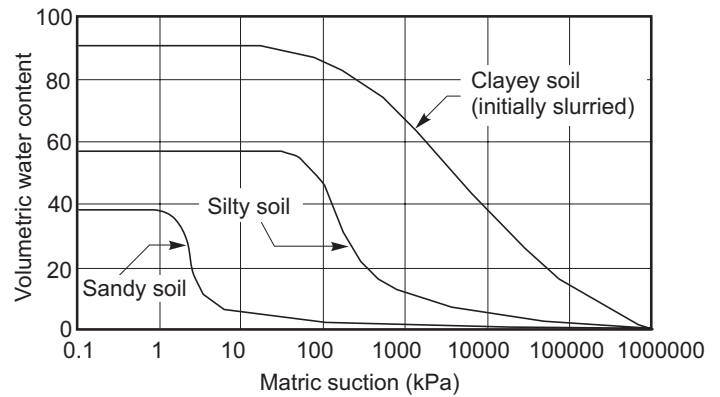


FIG. 2. Soil-water characteristic curves for sandy soil, a silty soil, and a clayey soil.

Literature review

Numerous empirical equations have been proposed to simulate the soil-water characteristic curve. Among the earliest is an equation proposed by Brooks and Corey (1964). It is in the form of a power-law relationship:

$$[1] \Theta = \left(\frac{\psi_b}{\psi} \right)^\lambda$$

where:

- Θ = normalized (or dimensionless) water content (i.e., $\Theta = (\theta - \theta_r)/(\theta_s - \theta_r)$, where θ_s and θ_r are the saturated and residual volumetric water contents, respectively),
- ψ = suction,
- ψ_b = air-entry value, and
- λ = pore-size distribution index.

The degree of saturation, S , has also been used in place of the normalized water content. Equation [1] has been verified through several studies (Campbell 1974; Clapp and Hornberger 1978; Gardner *et al.* 1970a, 1970b; Rogowski 1971; Williams *et al.* 1983; McCuen *et al.* 1981).

The following linear relationship between the logarithm of volumetric water content and the logarithm of suction was used by Williams *et al.* (1983) to describe the soil-water characteristic curve of many soils in Australia.

$$[2] \ln \psi = a_1 + b_1 \ln \theta$$

where: a_1 and b_1 = curve-fitting parameters.

McKee and Bumb (1984) suggested an exponential function for the relationship between the normalized water content and suction. This has been referred to as the Boltzmann distribution:

$$[3] \Theta = e^{-(\psi - a_2)/b_2}$$

where: a_2 and b_2 = curve-fitting parameters.

Equations [1] and [3] have been found to be valid for suction values greater than the air-entry value of the soil. The equations are not valid near maximum desaturation or under fully saturated conditions. To remedy this condition, McKee and Bumb (1987) and Bumb (1987) suggested the following relationship:

$$[4] \Theta = \frac{1}{1 + e^{(\psi - a_3)/b_3}}$$

where: a_3 and b_3 = curve-fitting parameters. This equation gives a better approximation in the low suction range. The

equation is not suitable in the high suction range, since the curve drops exponentially to zero at high suction values.

Equation [1] implies that there is a sharp discontinuity in suction near saturation. Although some coarse-grained sands may have a rapid change in suction at low suctions, most soils, particularly medium and fine textured soils, show a gradual curvature in the air-entry region near saturation. A modification of Eq. [1] was suggested by Roger and Hornberger (1978) to account for gradual air entry. In the case where the volumetric water content is referenced to zero water content and the normalized volumetric water content, Θ , (i.e., θ/θ_s), is plotted as the abscissa, the general soil-water characteristic plot has an inflection point where the slope, $d\psi/d\Theta$, changes from an increasing value to a decreasing value as Θ decreases. The inflection point is assigned the coordinates (Θ_i, ψ_i) , and the interval $\Theta_i \leq \Theta \leq 1$ can be described by a parabola:

$$[5] \psi = -a_4 (\Theta - b_4)(\Theta - 1)$$

where a_4 and b_4 = curve-fitting parameters. The parameters a_4 and b_4 are obtained by forcing Eq. [5] through the two points (Θ_i, ψ_i) and $(1, 0)$. The slopes of both Eq. [1] and Eq. [5] are equal at the inflection point.

Another frequently used form for the relationship between suction and the normalized water content was given by van Genuchten (1980):

$$[6] \Theta = \left[\frac{1}{1 + (p\psi)^n} \right]^m$$

where p , n , and m = three different soil parameters. This form of the equation gives more flexibility than the previous equations described. In an attempt to obtain a closed-form expression for hydraulic conductivity, van Genuchten (1980) related m and n through the equation $m = (1 - 1/n)$. This, however, reduces the flexibility of Eq. [6]. More accurate results can be obtained by leaving m and n parameters with no fixed relationship.

Gardner (1958) proposed an equation for the permeability function. The equation emulates the soil-water characteristic curve and can be visualized as a special case of Eq. [6]:

$$[7] \Theta = \frac{1}{1 + q\psi^n}$$

where:

q is a curve-fitting parameter related to the air-entry value of the soil, and

n is a curve-fitting parameter related to the slope at the inflection point on the soil-water characteristic curve.

Theoretical basis for the shape of the soil-water characteristic curve

The equations proposed in the research literature are empirical in nature. Each equation appears to apply for a particular group of soils. There are other equations of slightly differing forms that could be tested to assess their fit with experimental data. For example, the soil-water characteristic curve appears to have the form of the right-hand side of a normal-distribution curve. Therefore, the following equation can be used to approximate the soil-water characteristic curve:

$$[8] \Theta = a_5 e^{-(b_5 \psi)^m}$$

where a_5 , b_5 , and m = curve-fitting parameters. Equation [8]

is not suitable as a general form, although it might apply for some soils over a limited range of suction values.

To establish a theoretical basis for the soil-water characteristic curve, let us consider the pore-size distribution curve for the soil. The soil may be regarded as a set of interconnected pores that are randomly distributed. The pores are characterized by a pore radius, r , and described by a function $f(r)$, where $f(r) dr$ is the relative volume of pores of radius r to $(r + dr)$. In other words, $f(r)$ is the density of pore volume corresponding to radius r . Since $f(r) dr$ is the contribution of the pores of radius r to $(r + dr)$ that are filled with water, the volumetric water content can be expressed as:

$$[9] \theta(R) = \int_{R_{min}}^R f(r) dr$$

where:

$\theta(R)$ is volumetric water content when all the pores with radius less than or equal to R are filled with water, and R_{min} is minimum pore radius in the soil.

Let R_{max} denote the maximum pore radius. Then, for the saturated case:

$$[10] \theta(R_{max}) = \theta_s$$

The capillary law states that there is an inverse relationship between matric suction and the radius of curvature of the air-water interface. In other words, the air-water interface bears an inverse relationship to the pore size being desaturated at a particular suction:

$$[11] r = \frac{C}{\psi}$$

where $C = (2T \cos \phi)$, a constant, where T = surface tension of water, and ϕ is angle of contact between water and soil. Two particular suction conditions can be defined as follows:

$$[12] \psi_{max} = \frac{C}{R_{min}}$$

and

$$[13] \psi_{aev} = \frac{C}{R_{max}}$$

where:

ψ_{max} = the suction value corresponding to the minimum pore radius, and

ψ_{aev} = the air-entry suction value of the soil.

Using the capillary law, Eq. [9] can be expressed in terms of suction:

$$[14] \theta(\psi) = \int_{\psi_{max}}^{\psi} f\left(\frac{C}{h}\right) d\left(\frac{C}{h}\right) = \int_{\psi}^{\psi_{max}} f\left(\frac{C}{h}\right) \frac{C}{h^2} dh$$

where h is variable of integration, representing suction. Equation [14] is the general form describing the relationship between volumetric water content and suction. If the pore-size distribution, $f(r)$, of a soil is known, the soil-water characteristic curve can be uniquely determined by Eq. [14]. Several special cases are as follows:

(1) *Case of a constant pore size function* - The pore sizes are uniformly distributed, that is, $f(r) = A$, where A is a constant. It follows, from Eq. [14] that:

$$[15] \theta(\psi) = \int_{\psi}^{\psi_{max}} \frac{AC}{h^2} dh = AC \left(\frac{1}{\psi} - \frac{1}{\psi_{max}} \right) = \frac{B}{\psi} - D$$

where $B = AC$, a constant, and $D = AC/\psi_{max}$, a constant.

(2) Case where pore-size function varies inversely as r^2 - For the case of $f(r) = A/r^2$, the relationship between volumetric water content and suction is:

$$[16] \quad \theta(\psi) = \int_{\psi}^{\psi_{max}} \frac{Ah^2 C}{C^2 h^2} dh = B - D\psi$$

where $B = A\psi_{max}/C$, a constant, and $D = A/C$, a constant. Equation [16] represents a linear variation in the pore sizes. In other words, there is a linear relationship between volumetric water content and suction.

(3) Case where pore-size function varies inversely as $r^{(m+1)}$ - For the case of $f(r) = A/r^{(m+1)}$, where m is an integer, the relationship between volumetric water content and suction is:

$$[17] \quad \theta(\psi) = \int_{\psi}^{\psi_{max}} \frac{Ah^{m+1} C}{C^{m+1} h^2} dh = B - D\psi^m$$

where $B = A(\psi_{max})^m/(mC^m)$, a constant, and $D = A/(mC^m)$, a constant. The power-law relationship (i.e., Eq. [1]) proposed by Brooks and Corey (1964) is simply a special case of Eq. [17]. In other words, the Brooks and Corey (1964) power-law relationship is valid only when the pore-size distribution is close to the distribution $f(r) = A/r^{m+1}$.

To describe the soil-water characteristic curve over the entire suction range from 0 to 10^6 kPa, volumetric water content is referenced to zero water content (otherwise, the normalized water content becomes negative if θ is less than θ_r). In this case, the normalized water content Θ becomes θ/θ_s . Equation [14] suggests that the following integration form can be used as a general form to approximate the soil-water characteristic curve:

$$[18] \quad \theta(\psi) = \theta_s \int_{\psi}^{\infty} f(h) dh$$

where $f(h)$ is pore-size distribution as a function of suction. Equation [18] will generally produce a non-symmetrical S-shaped curve. Several special cases are as follows.

(1) Case of a normal distribution

Let us assume that $f(h)$ is a normal distribution. That is:

$$[19] \quad f(h) = \frac{1}{\sqrt{2\pi}\sigma} e^{-(h-\mu)^2/2\sigma^2}$$

where μ = mean value of the distribution of $f(h)$, and σ = standard deviation of the distribution of $f(h)$. The soil-water characteristic curve defined by Eq. [18] can be expressed as follows:

$$[20] \quad \begin{aligned} \theta(\psi) &= \theta_s \int_{\psi}^{\infty} f(h) dh \\ &= \frac{\theta_s}{2} \frac{2}{\sqrt{\pi}} \int_{(\psi-\mu)/\sqrt{2}\sigma}^{\infty} e^{-y^2} dy \\ &= \frac{\theta_s}{2} \operatorname{erfc}\left(\frac{\psi-\mu}{\sqrt{2}\sigma}\right) \end{aligned}$$

where:

$$\begin{aligned} \operatorname{erfc}(x) &= \frac{2}{\sqrt{\pi}} \int_x^{\infty} e^{-y^2} dy \\ &= 1 - \operatorname{erf}(x) = 1 - \frac{2}{\sqrt{\pi}} \int_0^{\infty} e^{-y^2} dy \end{aligned}$$

$\operatorname{erfc}(x)$ = complement of the error function $\operatorname{erf}(x)$. Equation [20] describes a symmetrical S-shaped curve. Therefore, if the pore-size distribution of a soil can be approximated by a normal distribution, the soil-water characteristic curve of the soil will be close to a symmetrical S-shaped curve, and Eq. [20] can be used as a model to describe this relationship.

The two fitting parameters (i.e., the mean value, μ , and the standard deviation, σ) in Eq. [20] are related to the air-entry value of the soil and the slope at the inflection point on the soil-water characteristic curve. If the slope at the inflection point is s and the air-entry value is ψ_{aev} , then the standard deviation, σ , can be written as:

$$[21] \quad \sigma = \frac{\theta_s}{\sqrt{2\pi} s}$$

and the mean value, μ , can be calculated as:

$$[22] \quad \mu = \psi_{aev} + \frac{\theta_s}{2s}$$

(2) Case of a gamma distribution

Consider the case of a gamma-type distribution for the function $f(r)$. That is, $f(h)$ takes the following form:

$$[23] \quad f(h) = \begin{cases} \frac{h^{\alpha-1} e^{-h/\beta}}{\beta^{\alpha} \Gamma(\alpha)}, & \alpha, \beta > 0, \quad 0 \leq h < \infty \\ 0, & \text{elsewhere} \end{cases}$$

where:

$$\Gamma(\alpha) = \int_0^{\infty} h^{\alpha-1} e^{-h} dh$$

In this case, the soil-water characteristic curve defined by Eq. [18] has a smaller air-entry value, a steeper slope near saturation, and a gentler slope near the residual water content. In the special case when α is an integer, the soil-water characteristic curve defined by Eq. [18] becomes:

$$[24] \quad \begin{aligned} \theta(\psi) &= \theta_s \int_{\psi}^{\infty} \frac{h^{\alpha-1} e^{-h/\beta}}{\beta^{\alpha} \Gamma(\alpha)} dh \\ &= \frac{\theta_s}{\Gamma(\alpha)} \int_{\psi/\beta}^{\infty} h^{\alpha-1} e^{-h} dh \\ &= \theta_s \sum_{i=0}^{\alpha-1} \frac{\psi^i e^{-\psi/\beta}}{i! \beta^i} \end{aligned}$$

For $\alpha = 1$, the gamma distribution becomes an exponential distribution:

$$[25] \quad f(h) = \begin{cases} \frac{1}{\beta} e^{-h/\beta}, & \beta > 0, \quad 0 \leq h < \infty \\ 0, & \text{elsewhere} \end{cases}$$

and the soil-water characteristic curve defined by Eq. [18] can be

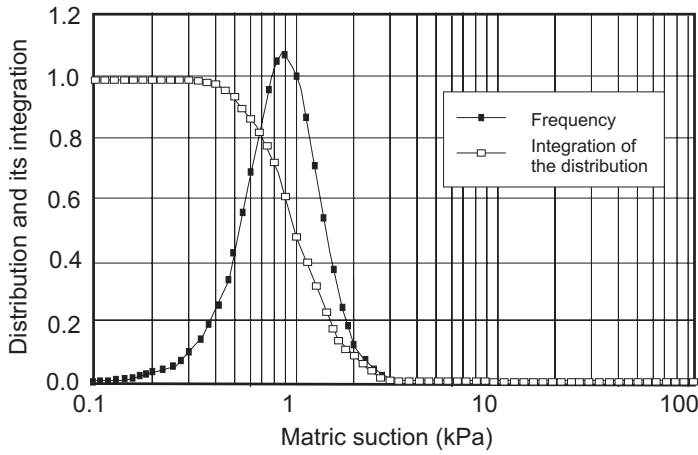


FIG. 3. A sample distribution using [29] and its integration (eg. [6]).

written as:

$$[26] \quad \theta(\psi) = \theta_s e^{-\psi/\beta}$$

Note that Eq. [26] has the same form as Eq. [3], which was used by McKee and Bumb (1984) to describe the soil-water characteristic curve. Therefore, Eq. [3] gives the best results if the pore-size distribution of the soil is close to a gamma distribution.

(3) Case of a beta distribution

Consider the case of a beta distribution for the function $f(r)$:

$$[27] \quad f(h) = \begin{cases} \frac{h^{\alpha-1} (1-h)^{\beta-1}}{B(\alpha, \beta)}, & \alpha, \beta > 0, \quad 0 \leq h \leq 1 \\ 0, & \text{elsewhere} \end{cases}$$

where:

$$B(\alpha, \beta) = \int_0^1 h^{\alpha-1} (1-h)^{\beta-1} dh = \frac{\Gamma(\alpha) \Gamma(\beta)}{\Gamma(\alpha + \beta)}$$

In this case, the soil-water characteristic curve given by Eq. [18] has greater flexibility. For α equal to β , Eq. [18] generates a symmetrical S-shaped curve. For α greater than β , the curve is non-symmetrical and has a higher air-entry value, a gentler slope near saturation, and a steeper slope near the residual water content. For α less than β , the curve has a smaller air-entry value, a steeper slope near saturation, and a gentler slope near the residual water content. In the case when α and β are integers, the soil-water characteristic curve defined by Eq. [18] and Eq. [27] is related to the binomial probability function as follows (Mendenhall *et al.* 1981):

$$[28] \quad \begin{aligned} \theta(\psi) &= \theta_s \int_{\psi}^1 \frac{h^{\alpha-1} (1-h)^{\beta-1}}{B(\alpha, \beta)} dh \\ &= \theta_s - \theta_s \sum_{i=\alpha}^{\alpha+\beta-1} \binom{\alpha+\beta-1}{i} \psi^i (1-\psi)^{\alpha+\beta-1-i} \end{aligned}$$

Equation [28] has a form similar to that of Eq. [5] suggested by Roger and Homberger (1978), which was used to account for a gradual air entry. Note, that defining r over the interval (0, 1) does not restrict its use. The beta density function can be applied to any interval by translation and a change in the scale.

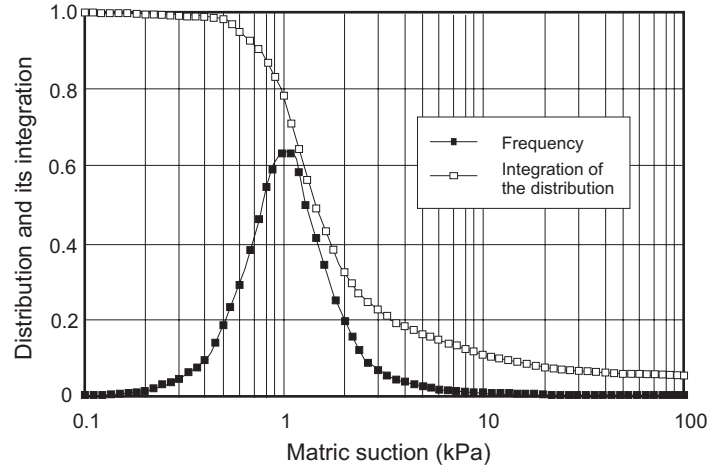


FIG. 4. A sample distribution using [30] and its integration.

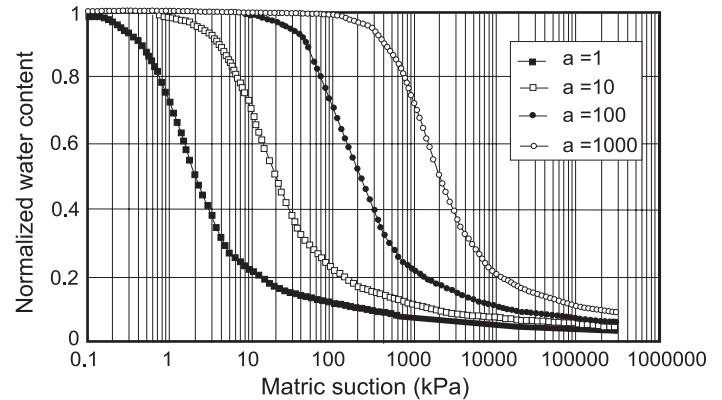


FIG. 5. Sample plots of [31] with $n = 2$ and $m = 1$ (a varies).

Proposal for a new equation

The pore-size distribution of Eq. [6] can be written as follows:

$$[29] \quad f(\psi) = \frac{mnp(p\psi)^{n-1}}{[1+(p\psi)^n]^{m+1}}$$

Figure 3 shows a sample probability distribution for Eq. [29] along with its integration (i.e., Eq. [6]). It can be seen that the integration drops to zero over a narrow suction range. Therefore, Eq. [6] is not suitable in the high suction region. Experimental data show that after the residual water content, the plot should decrease linearly to a value of about 10^6 kPa (Croney and Coleman 1961). To describe the soil-water characteristic curve more accurately, the following distribution is suggested:

$$[30] \quad f(\psi) = \frac{mn(\psi/a)^{n-1}}{a[e+(\psi/a)^n] \{ \log[e+(\psi/a)^n] \}^{m+1}}$$

Equation [30] and its integration form are shown in Fig. 4 for the same set of parameters (i.e., $a = 1/p, n, m$). This distribution function drops more slowly than Eq. [29] as ψ increases and, therefore, Eq. [30] produces a nonsymmetrical curve that is closer to the experimental data.

Integrating Eq. [30] using Eq. [18] gives the following relationship between volumetric water content and suction:

$$[31] \quad \theta = \theta_s \left[\frac{1}{\ln[e+(\psi/a)^n]} \right]^m$$

Figures 5 to 7 show the effect of varying the three parameters a, n , and m on the shape of the soil-water characteristic

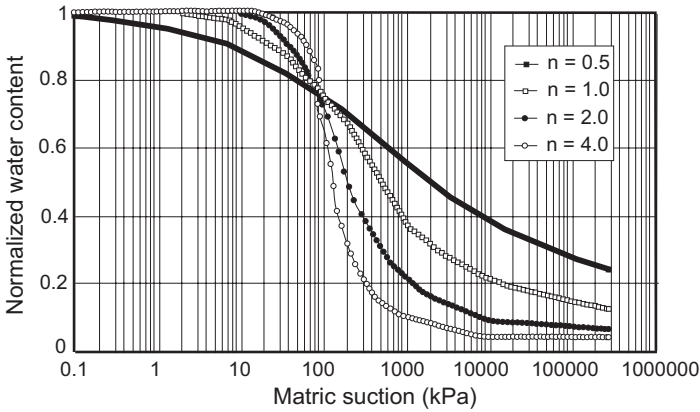


FIG. 6. Sample plots of [31] with $a = 100$ and $m = 1$ (n varies).

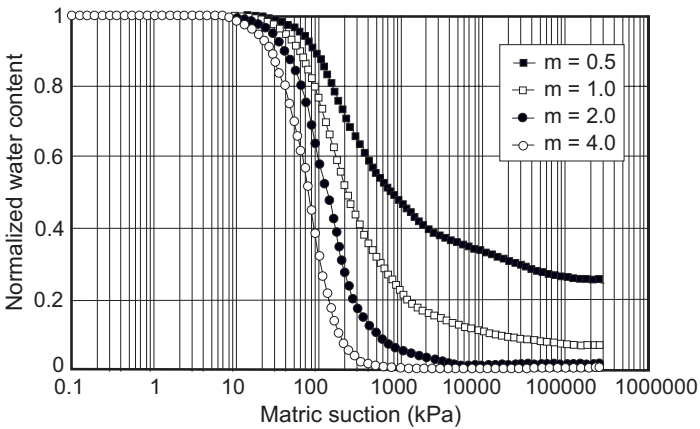


FIG. 7. Sample plots of [31] with $a = 100$ and $n = 2$ (m varies).

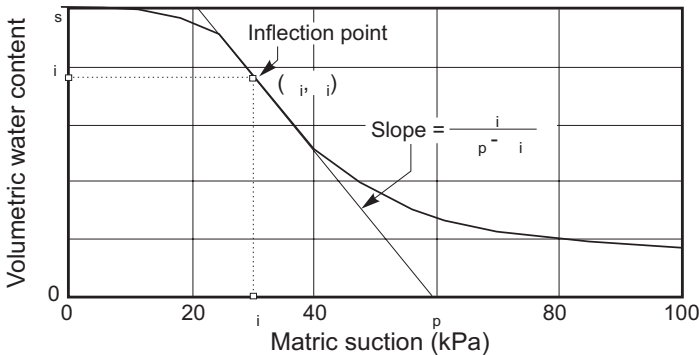


FIG. 8. A sample plot for the graphical solution of the three parameters (a , n , and m) in [31].

curve. From Fig. 5 it can be seen that when n and m are fixed, the parameter a (with a unit of kPa) is closely related to the air-entry value. In general, the value for the parameter a would be higher than the air-entry value. However, for small values of m , the air-entry value can be used for parameter a .

Figure 6 indicates that parameter n controls the slope of the soil-water characteristic curve. The distribution given by Eq. [30] attains its maximum value approximately at the value of a . Therefore, the point $(a, \theta(a))$ can be used to approximate the inflection point. Using this information, a graphical estimation for the three parameters can be obtained from the soil-water characteristic curve. First, locate the inflection point (ψ_p, θ_i) on the soil-water characteristic plot and draw a tangent line through this point (Fig. 8).

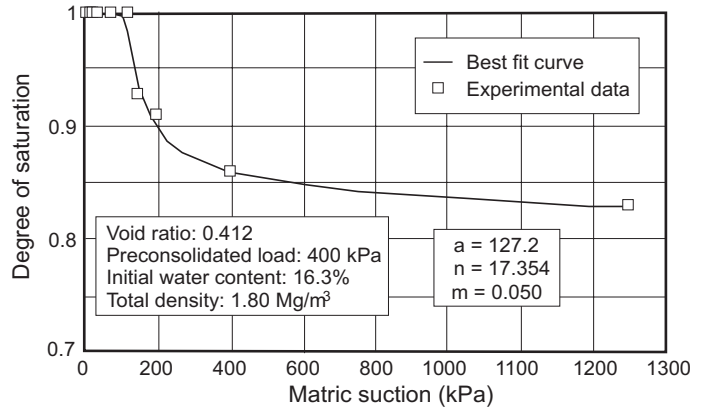


FIG. 9. A best-fit curve to the experimental data of a till (S. Vanapalli, personal communication, 1993).

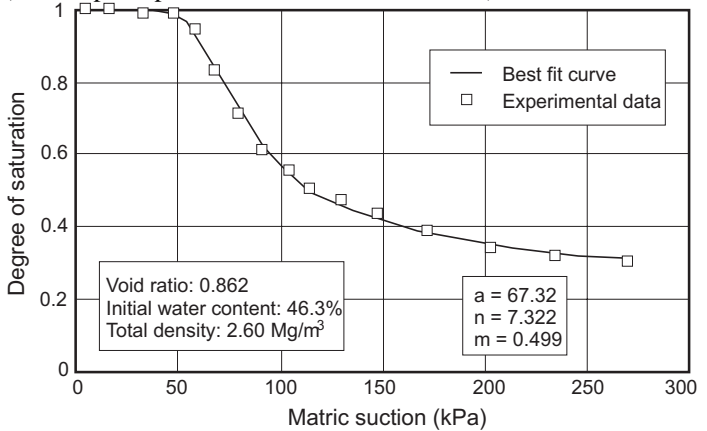


FIG. 10. A best-fit curve to the experimental data of a silty loam (data from Brooks and Corey 1964).

Let s denote the slope of the tangent line. Then, the three parameters a , n , and m are determined as follows:

$$[32] \quad a = \psi_i$$

$$[33] \quad m = 3.67 \ln \left(\frac{\theta_s}{\theta_i} \right)$$

$$[34] \quad n = \frac{1.31^{m+1}}{m\theta_s} 3.72 s \psi_i$$

The slope, s , of the tangent line can be calculated as:

$$[35] \quad s = \frac{\theta_i}{\psi_p - \psi_i}$$

where ψ_p = intercept of the tangent line and the matric suction axis (Fig. 8).

Small values of m result in a moderate slope in the high-suction range, and large values of n produce a sharp corner near the air-entry value (see Fig. 9). Another example of a best-fit curve to the experimental data for a silty loam from Brooks and Corey (1964) is shown in Fig. 10.

In Eq. [31], θ becomes equal to θ_s when the suction is zero, and θ becomes zero when the suction goes to infinity. It is also possible to use the degree of saturation for curve fitting, since the degree of saturation varies from 0 to 1. Gravimetric water content can be similarly normalized for curve-fitting purpose. Three plots are shown for the same soil (i.e., silty

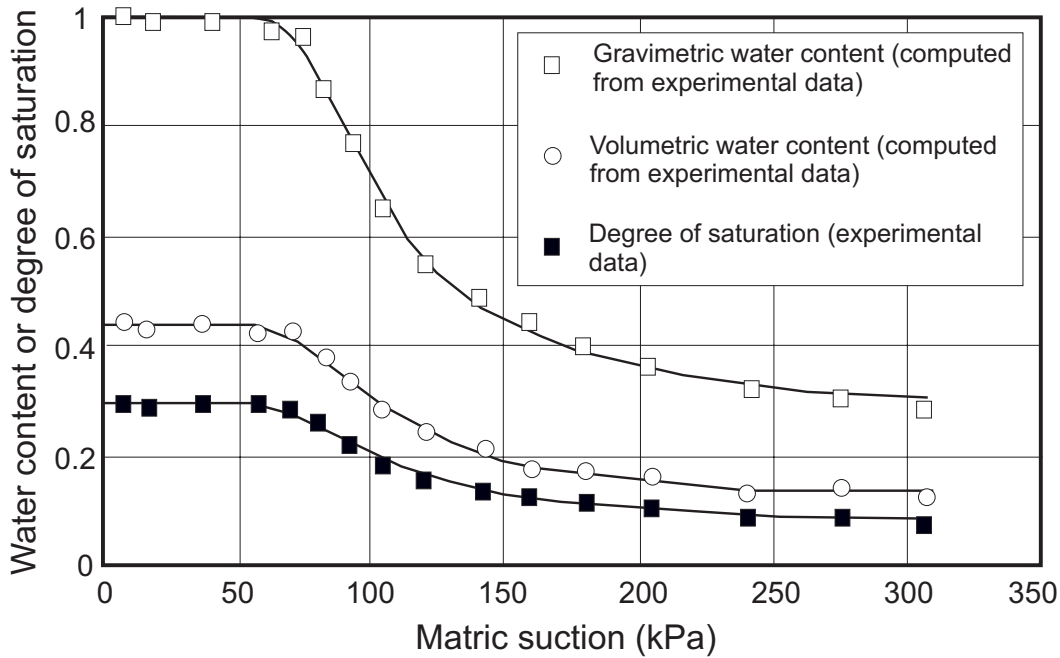


FIG. 11. Best-fit curves to the experimental data of a silty loam using three different representations of the water content, i.e., degree of saturation, volumetric water content, and gravimetric water content (data from Brooks and Corey 1964).

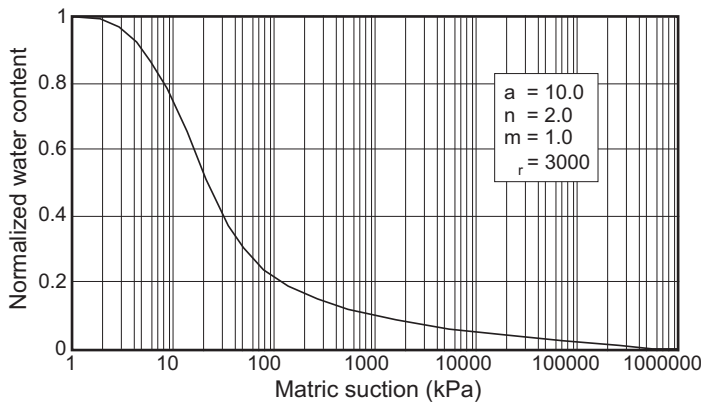


FIG. 12. A sample plot of [36].

loam) in Fig. 11, using different ways of representing the water content of the soil (i.e., degree of saturation, volumetric water content, and gravimetric water content).

Experimental data have previously shown that the suction of a soil reaches a maximum value of approximately 10^6 kPa at zero water content. This upper limit can be built into Eq. [31] as follows:

$$[36] \quad \theta(\psi, a, n, m) = C(\psi) \frac{\theta_s}{\left\{ \ln \left[e + (\psi/a)^n \right] \right\}^m}$$

where $C(\psi)$ is a correction function defined as

$$C(\psi) = \frac{-\ln(1 + \psi/\psi_r)}{\ln[1 + (1,000,000/\psi_r)]} + 1$$

where ψ_r = suction corresponding to the residual water content, θ_r .

It can be seen that $C(1,000,000)$ is equal to zero. Therefore, at the limiting point where ψ is equal to 10^6 kPa, the water content, θ , calculated from Eq. [36] is zero. A sample plot for Eq. [36] is shown in Fig. 12. The curve at the low-suction range is not

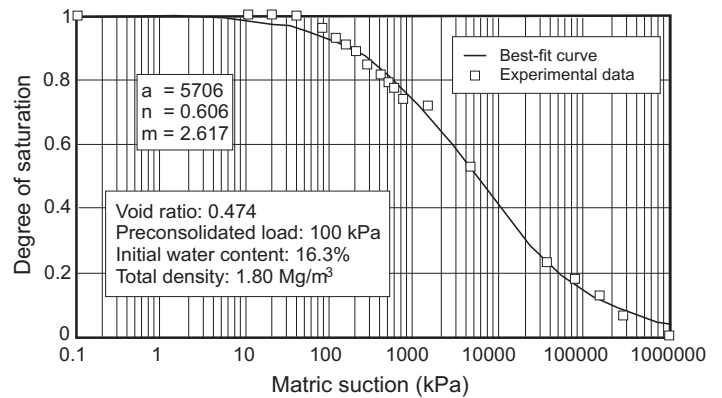


FIG. 13. A best-fit curve to the experimental data of a till using [31] (S. Vanapalli, personal communication, 1993).

significantly affected, since the correction function $C(\psi)$ is approximately equal to 1 at low suctions.

Figure 13 shows a best-fit curve to the experimental data obtained for a glacial till, using Eq. [31]. A best-fit curve to the same experimental data using Eq. [36] is shown in Fig. 14. It can be seen that the modified equation (i.e., Eq. [36]) fits the data better than Eq. [31]. The main difference is that the curve is forced by $C(\psi)$ to zero at a suction of 10^6 kPa.

A graphical estimation of the four parameters a , n , m , and ψ_r , in Eq. [36] can be obtained from a semilog plot of the soil-water characteristic curve. First, determine the suction corresponding to the residual water content ψ_r by locating a point where the curve starts to drop linearly in the high suction range (Fig. 15). Numerical results show that, in most cases, Eq. [36] gives a satisfactory approximation for $\psi_r > 1500$ kPa. Its magnitude will generally be in the range of 1500 to 3000 kPa. Figure 15 uses ψ_r equal to 3000 kPa for illustration purposes. Next, locate the inflection point (ψ_i , θ_i) on the semilog plot and draw a tangent line through this point

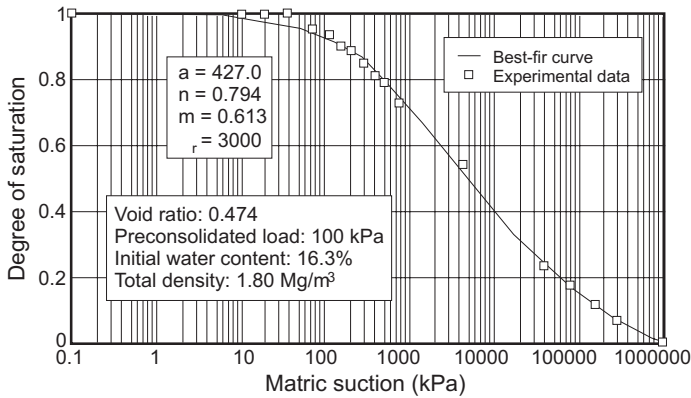


FIG. 14. A best-fit curve to the experimental data in Fig. 13 using [36].

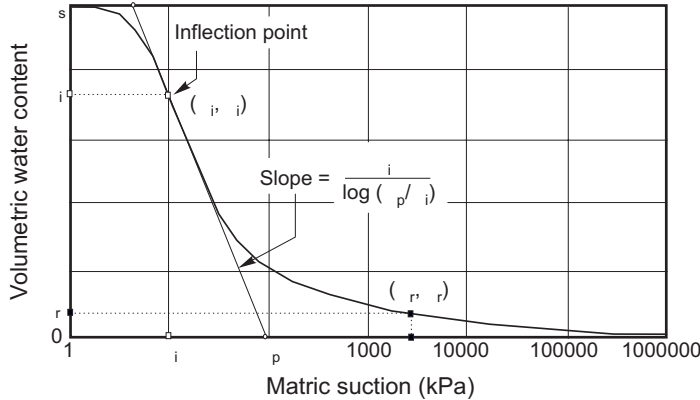


FIG. 15. A sample plot for the graphical solution of the four parameters (a , n , m , and ψ_i) in [36].

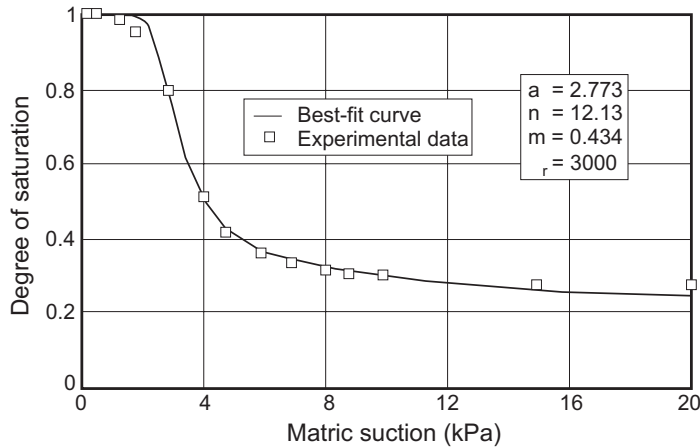


FIG. 16. A best-fit curve to the experimental data of a sand (data from Moore 1939).

(Fig. 15). Let s denote the slope of the tangent line on the semilog plot. Then, the fitting parameters a , n , and m can be determined as follows:

$$[37] \quad a = \psi_i$$

$$[38] \quad m = 3.67 \ln \left[\frac{\theta_s C(\psi_i)}{\theta_i} \right]$$

$$[39] \quad n = \frac{1.31^{m+1}}{mC(\psi_i)} 3.72 s^*$$

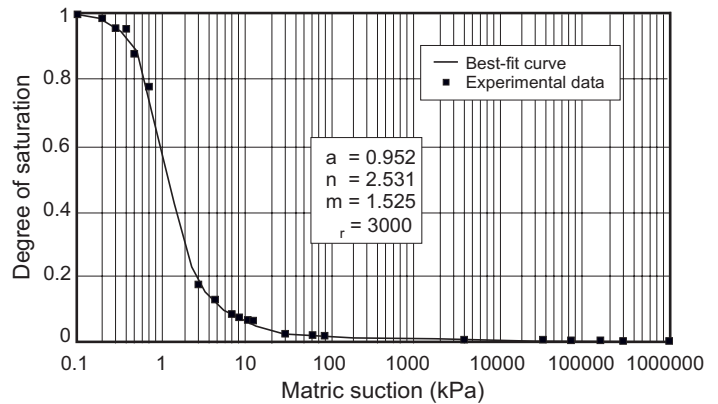


FIG. 17. A best-fit curve to the experimental data of a sand (Soil Laboratory data, University of Saskatchewan).

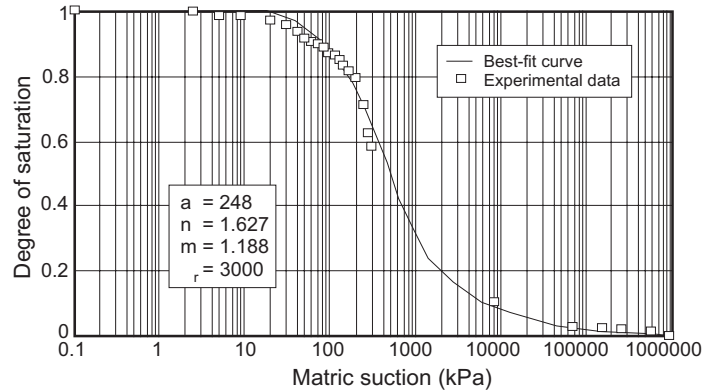


FIG. 18. A best-fit curve to the experimental data of Kidd Creek tailings (N. Yang, personal communication, 1992).

where:

$$s^* = \frac{s}{\theta_s} - \frac{\psi_i}{1.31^m (\psi_i + \psi_r) \ln [1 + (1,000,000 / \psi_r)]}$$

The slope, s , of the tangent line can be calculated as follows:

$$[40] \quad s = \frac{\theta_i}{\ln(\psi_p / \psi_i)}$$

where ψ_p = intercept of the tangent line on the semilog plot and the matric suction axis (Fig. 15).

A graphical estimation only gives approximate values for the parameters. To obtain a closer fit to experimental data, the three parameters (a , n , and m) in Eq. [36] can be determined using a least squares method, if the measured data for θ and ψ are available. The idea is to choose the three parameters such that the calculated values from Eq. [36] are as close as possible to the measured values. Therefore, the following objective function (i.e., sum of the squared deviations of the measured data from the calculated data) is minimized with respect to the three parameters a , n , and m .

$$[41] \quad O(a, m, n) = \sum_{i=1}^M [\theta_i - \theta(\psi_i, a, m, n)]^2$$

where:

$O(a, m, n)$ is the objective function,
 M is the total number of measurements, and
 θ_i and ψ_i are measured values.

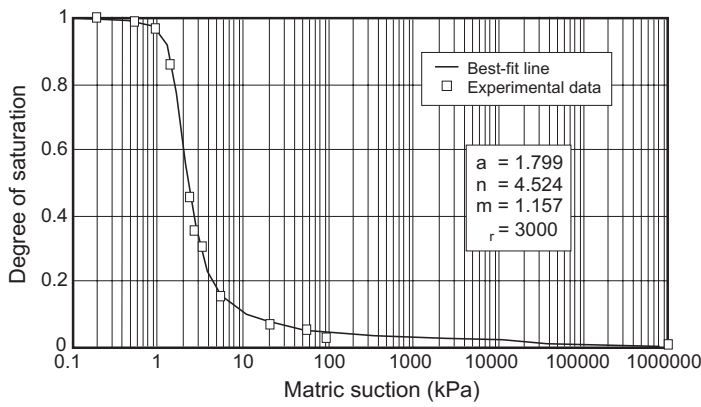


FIG. 19. A best-fit curve to the experimental data of a sand (Soil Laboratory data, University of Saskatchewan).

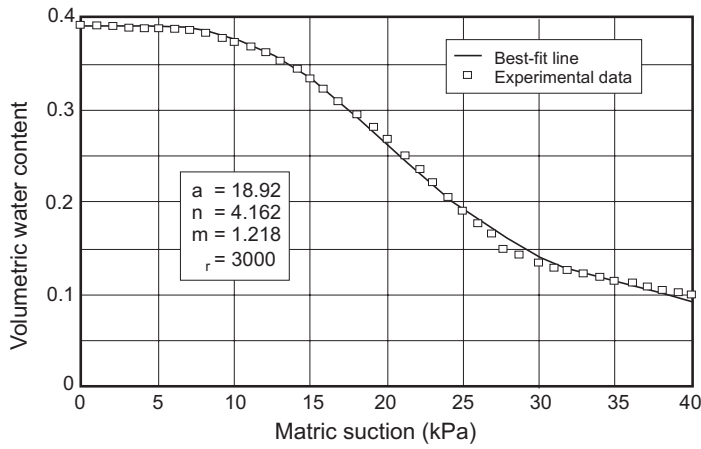


FIG. 20. A best-fit curve to the experimental data of a sand (University of Toronto data; University of Saskatchewan 1984).

This is a non-linear minimization problem. A curve-fitting utility CFVIEW was coded based on Eq. [36] and Eq. [41] using a quasi-Newton method. The detailed non-linear curve-fitting algorithm is presented in the Appendix. Best-fit curves for a tailings sand, a silt, and a clay are shown in Figs. 16 to 23. An arithmetic scale has been used when the experimental data in the high suction range are not available. It can be seen, from these results, that Eq. [36] can be used to fit the experimental data reasonably well over the entire suction range of 0 to 10⁶ kPa.

Some applications require an estimation of the residual water content. The following slightly different form of Eq. [31] can be used to estimate the residual water content θ_r :

$$[42] \quad \theta = \theta_r + \frac{\theta_s - \theta_r}{\left\{ \ln \left[e + (\psi / a)^n \right] \right\}^m}$$

Here, θ_r and θ_s are treated as two additional parameters. The five parameters a , n , m , θ_r , and θ_s , in Eq. [42] can be systematically identified through a best-fit analysis on experimental data.

Conclusions

General empirical equations have been proposed to describe the soil-water characteristic curve. Each equation has its own limitations. A general form of the relationship between water content and suction was developed based on the pore-size dis-

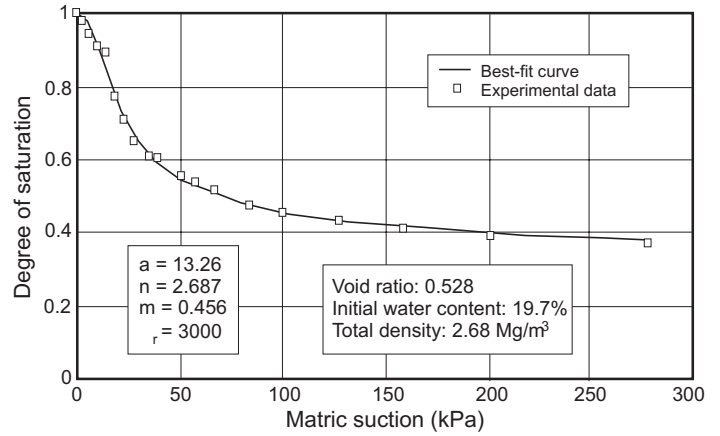


FIG. 21. A best-fit curve to the experimental data of a silt (S. Huang, personal communication, 1993).

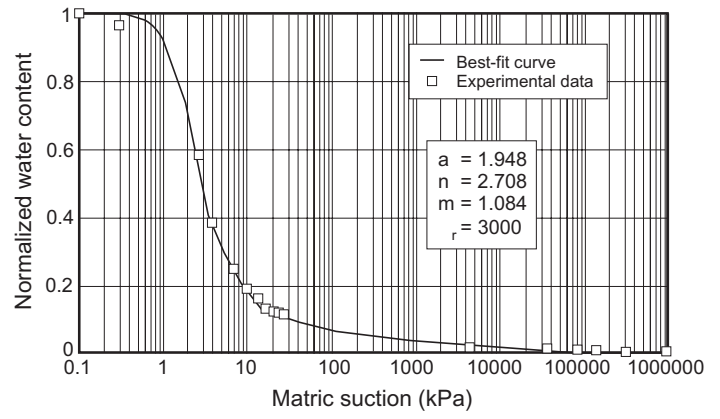


FIG. 22. A best-fit curve to the experimental data of a silt (Soil Laboratory data, University of Saskatchewan).

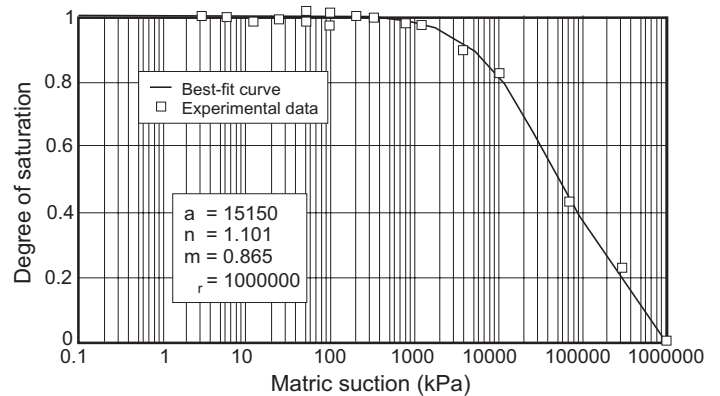


FIG. 23. A best-fit curve to the experimental data of an initially slurred Regina clay (data from Fredlund).

tribution of the soil. If the pore-size distribution of a soil can be obtained or predicted, then the soil-water characteristic curve is uniquely determined from the proposed general equation.

The analysis in this paper provides not only a theoretical basis for most of the empirical equations but also proposes a new, more general equation to describe the soil-water characteristic curve. Based on the proposed equation, a curve-fitting utility, CFVIEW, was coded. It was found that the equation fits experimental data reasonably well over the entire suction range from 0 to 10⁶ kPa.

Acknowledgement

The authors would like to thank Sai Vanapalli for supplying experimental data and for helpful suggestions for the curve-fitting program.

- Brooks, R.H., and Corey, A.T. 1964. Hydraulic properties of porous medium. Colorado State University (Fort Collins), Hydrology Paper, Nr. 3, March.
- Bumb, A.C. 1987. Unsteady-state flow of methane and water in coalbeds. Ph.D. thesis, Department of Chemical Engineering, University of Wyoming, Laramie.
- Campbell, G.S. 1974. A simple method for determining unsaturated conductivity from moisture retention data. *Soil Science*, **117**: 311-314.
- Clapp, R.B., and Hornberger, G.M. 1978. Empirical equations for some soil hydraulic properties. *Water Resources Research*, **14**: 601-604.
- Croney, D., and Coleman, J.D. 1961. Pore pressure and suction in soils. *Proceedings, Conference on Pore Pressure and Suction in Soils*. Butterworths, London. pp. 31-37.
- Fredlund, D.G. 1964. Comparison of soil suction and one-dimensional consolidation characteristics of a highly plastic clay. M.Sc. thesis, Department of Civil Engineering, University of Alberta, Edmonton, AB, Canada.
- Fredlund, D.G., and Rahardjo, H. 1993a. Soil mechanics for unsaturated soils. John Wiley & Sons, Inc., New York.
- Fredlund, D.G., and Rahardjo, H. 1993b. An overview of unsaturated soil behaviour. *Proceedings, ASCE Specialty Series on Unsaturated Soil Properties*, Dallas, TX., October 24-28, pp. 1-33.
- Gardner, W.R. 1958. Some steady state solutions of the unsaturated moisture flow equation with application to evaporation from a water-table. *Soil Science*, **85**: 228-232.
- Gardner, W.R., Hillel D., and Benyamini, Y. 1970a. Post irrigation movement of soil water. I. Redistribution. *Water Resources Research*, **6**: 851-861.
- Gardner, W.R., Hillel D., and Benyamini, Y. 1970b. Post irrigation movement of soil water. II. Simultaneous redistribution and evaporation. *Water Resources Research*, **6**: 1148-1153.
- Marshall, T.J. 1958. A relation between permeability and size distribution of pores. *Journal of Soil Science*, **9**: 1-8.
- McCuen, R.H., Rawls, W.J., and Brakensiek, D.L. 1981. Statistical analyses of the Brook-Corey and the Green-Ampt parameters across soil textures. *Water Resources Research*, **17**: 1005-1013.
- McKee, C.R., and Bumb, A.C. 1984. The importance of unsaturated flow parameters in designing a monitoring system for hazardous wastes and environmental emergencies. *Proceedings, Hazardous Materials Control Research Institute National Conference*, Houston, TX, March 1984. pp. 50-58.
- McKee, C.R., and Bumb, A.C. 1987. Flow-testing coalbed methane production wells in the presence of water and gas. *In SPE Formation Evaluation*, December, pp. 599-608.
- Mendenhall, W., Scheaffer, R.L., and Wackerly, D.D. 1981. *Mathematical statistics with applications*. 2nd Edition. Duxbury Press, Boston.
- Moore, R.E. 1939. Water conduction from shallow water tables. *Hilgardia*, **12**: 383-426.
- Mualem, Y. 1986. Hydraulic conductivity of unsaturated soils: prediction and formulas. *In Methods of soil analysis. Part I Physical and mineralogical methods*. 2nd Edition. Agronomy. Edited by A. Klute. American Society of Agronomy, Inc. and Soil Society of America, Inc., Madison, Wis., U.S.A., pp. 799-823.
- Papagiannakis, A.T., and Fredlund, D.G. 1984. A steady state model for flow in saturated-unsaturated soils. *Canadian Geotechnical Journal*, **21**: 419-430.
- Richards. B.G. 1965. Measurement of the free energy of soil moisture by the psychrometric technique using thermistors. *In Moisture equilibria and moisture changes in soils beneath covered areas*. Edited by G.D. Aitchison. Butterworth & Co. Ltd., Sydney, Australia, pp. 39-46.
- Roger, B.C., and Hornberger, G.M. 1978. Empirical equations for some soil hydraulic properties. *Water Resources Research*, **14**:601-604.
- Rogowski, A.S. 1971. Watershed physics: model of the soil moisture characteristic. *Water Resources Research*, **7**: 1575-1582.
- Sadler, D.R. 1975. *Numerical methods for nonlinear regression*. University of Queensland Press, St. Lucia, Queensland, Australia.
- University of Saskatchewan. 1984. *KCAL User's manual*. A computer program for calculating unsaturated permeability. Department of Civil Engineering, University of Saskatchewan. Saskatoon.
- van Genuchten, M.T. 1980. A closed-form equation for predicting the hydraulic conductivity of unsaturated soils. *Soil Science Society of America Journal*, **44**: 892-898.
- Williams, P.J. 1982. *The surface of the Earth, an introduction to geotechnical science*. Longman Inc., New York.
- Williams, J., Prebble, R.E., Williams, W.T., and Hignett, C.T. 1983. The influence of texture, structure and clay mineralogy on the soil moisture characteristic. *Australian Journal of Soil Research*, **21**: 15-32.

Appendix: Nonlinear curve-fitting algorithms for the soil-water characteristic curve

The proposed equation for the soil-water characteristic curve is:

$$[A1] \quad \theta(\psi, a, n, m) = C(\psi) \frac{\theta_s}{\left\{ \ln \left[e + (\psi / a)^n \right] \right\}^m}$$

Let $p = (a, n, m)$ denote the unknown vector of the three parameters a , n , and m and suppose that measured data (θ_i, ψ_i) ($i = 1, 2, \dots, M$) are available, where M is the number of measurements. The least squares estimate of p is the vector p^* , which minimizes the following objective function (i.e., sum of the squared deviations of the measured data from the calculated data).

$$[A2] \quad O(p) = O(a, m, n) = \sum_{i=1}^M [\theta_i - \theta(\psi_i, a, m, n)]^2$$

In other words, the least squares method determines the three parameters such that the calculated values from Eq. [A1] are as close as possible to the measured values.

A standard requirement of iterative minimization algorithms is that the value of the objective function decreases monotonically from iteration to iteration. Let p_i be the estimate of p at the beginning of the i th iteration (p_0 is the initial guess and, theoretically, it is arbitrary). The new estimate p_{i+1} is chosen such that

$O(p_{i+1}) < O(p_i)$. The steepest descent method is one of the easiest methods for minimizing a general nonlinear function of several variables. It exploits the fact that from a given starting point a function decreases most rapidly in the direction of the negative gradient vector evaluated at the starting point. Let g denote the gradient of $O(p)$ at p_i . That is:

$$[A3] \quad g = \left[\begin{array}{c} \frac{\partial O(p)}{\partial a} \\ \frac{\partial O(p)}{\partial n} \\ \frac{\partial O(p)}{\partial m} \end{array} \right]_{p=p_i}$$

The steepest descent iteration is defined by

$$[A4] \quad p_{i+1} = p_i - \alpha g$$

where α = scalar that determines the length of the step taken in the direction of $-g$.

From Eq. [A2] it follows that:

$$[A5] \quad \frac{\partial O(p)}{\partial a} = -2 \sum_{i=1}^M [\theta_i - \theta(\psi_i, a, n, m)] \frac{\partial \theta(\psi_i, a, n, m)}{\partial a}$$

Similarly,

$$[A6] \quad \frac{\partial O(p)}{\partial n} = -2 \sum_{i=1}^M [\theta_i - \theta(\psi_i, a, n, m)] \frac{\partial \theta(\psi_i, a, n, m)}{\partial n}$$

$$[A7] \quad \frac{\partial O(p)}{\partial m} = -2 \sum_{i=1}^M [\theta_i - \theta(\psi_i, a, n, m)] \frac{\partial \theta(\psi_i, a, n, m)}{\partial m}$$

From Eq. [A1], the partial derivatives in Eqs. [A5] to [A7] can be obtained as follows:

$$[A8] \quad \frac{\partial \theta(\psi_i, a, n, m)}{\partial a} = mC(\psi_i)\theta_s \left\{ \ln[e + (\psi_i/a)^n] \right\}^{-m-1} \frac{n(\psi_i/a)^{n-1}(\psi_i/a^2)}{e + (\psi_i/a)^n}$$

$$[A9] \quad \frac{\partial \theta(\psi_i, a, n, m)}{\partial n} = -mC(\psi_i)\theta_s \left\{ \ln[e + (\psi_i/a)^n] \right\}^{-m-1} \frac{(\psi_i/a)^n \ln(\psi_i/a)}{e + (\psi_i/a)^n}$$

$$[A10] \quad \frac{\partial \theta(\psi_i, a, n, m)}{\partial m} = -C(\psi_i)\theta_s \left\{ \ln[e + (\psi_i/a)^n] \right\}^{-m} \ln \left\{ \ln[e + (\psi_i/a)^n] \right\}$$

The steepest descent method is not efficient for practical use, since the rate of convergence is slow, especially near the stationary point. The following quasi-Newton method (Sadler 1975) was used for the curve-fitting program:

$$[A11] \quad p_{i+1} = p_i - A_i g_i$$

where:

g_i = gradient of the objective function evaluated at p_i , and

A_i = operative matrix at the i -th iteration.

Equation [A11] becomes the steepest descent method if A_i is the identity matrix multiplied by a step length (a scalar). Denote $p_{i-1} - p_i$ by d_i and $g_{i+1} - g_i$ by q_i . Then A_i is updated using the following formula:

$$[A12] \quad A_{i+1} = A_i + \frac{(d_i - A_i q_i)(d_i - A_i q_i)^T}{(d_i - A_i q_i)^T q_i}$$

where the superscript T denotes the transpose of a vector matrix.

A suitable choice for A_0 is the diagonal matrix defined by:

$$[A13] \quad a_{ij} = \begin{cases} \frac{\alpha_i}{2\beta_i} & \text{if } i = j \\ 0 & \text{if } i \neq j \end{cases}$$

where:

α_i = i -th element of the starting vector p_0 ,

β_i = i -th element of the gradient g_0 evaluated at the starting vector.

The quasi-Newton method does not require matrix inversion or equivalent, since the sequence A_i ($i = 0$,

1, 2, ...) converges to the inverse Hessian. In practice, the objective function is often approximately quadratic near the minimum, so a second-order convergence can be eventually expected. However, there is no guarantee that A_i remain positive definite, even for a quadratic function. The product $g_i^T d_i$ should be checked and d_i replaced by its negative, if $g_i^T d_i > 0$. Numerical difficulties may also arise when the scalar product $(d_i - A_i q_i)^T q_i$ is very small, resulting in unduly large elements in A_{i+1} . One of several possible strategies is to reinitialize A_{i+1} if the cosine of the angle between $(d_i - A_i q_i)$ and q_i is less than 0.0001. For a nonquadratic objective function it is reasonable to adjust the step length so that the objective function is reduced at each iteration.